Available online at www.sciencedirect.com

jmr&t Journal of Materials Research and Technology

journal homepage: www.elsevier.com/locate/jmrt

Original Article

Electroactive shaping and shape memory of sequential dual-cured off-stoichiometric epoxy/CNT composites

S.G. Prolongo [a,*], C.G. Díaz-Maroto [b,c], A. Jiménez-Suárez [a]

[a] Materials Science and Engineering Area, University Rey Juan Carlos, C/Tulipán s/n, 28933, Móstoles, Madrid, Spain
[b] Chemical and Environmental Engineering Group, University Rey Juan Carlos, C/Tulipán s/n, 28933, Móstoles, Madrid, Spain
[c] Thermochemical Processes Unit, IMDEA Energy, Avda. Ramón de La Sagra 3, 28935, Móstoles, Madrid, Spain

ARTICLE INFO

Article history:
Received 27 May 2021
Accepted 23 September 2021
Available online 28 September 2021

Keywords:
Sequential dual curing
Epoxy nanocomposite
Carbon nanotubes
Shape memory
Joule heating

ABSTRACT

Sequential dual-cured epoxy composites, based on off-stoichiometric thiol–epoxy mixtures catalysed by 1-methylimidazole, have been developed by adding carbon nanotubes (CNT). The epoxy curing process initially consists in two thermally activated curing stages: a first thiol–epoxy reaction and later homopolymerization at a higher temperature. This system presents easy shaping/conforming and shape memory properties through thermo-mechanical treatments. Addition of the electrical CNT network into the epoxy matrix allows electrical switching, which increases its performance and in-situ applicability.

The obtained results confirmed that CNTs catalyse the homopolymerization epoxy reaction, hindering the sequential curing process, due to the π–π anchoring of imidazole catalyser over the CNTs surface, enhanced by donor–acceptor interaction.

Non-doped off-stoichiometric resins present relatively high thermal strength, with a glass transition temperature in the range of 73–109 °C, and high stiffness, with a storage modulus close to 2–3 GPa. They can be easily conformed at low temperature, 60 °C, before their second curing stage, showing a high shaping efficiency (around 90%) and full fixing efficiency (>98%).

Nanocomposites with 0.2% CNT present efficient Joule heating, triggering the shape memory at low voltage, <80 V, with fixing and recovery efficiencies of 60–85%. In addition to its high in-situ applicability, the electrical resistive heating is faster and more efficient than conventional heating in an oven.

* Corresponding author.
E-mail address: silvia.gonzalez@urjc.es (S.G. Prolongo).

https://doi.org/10.1016/j.jmrt.2021.09.102

1. Introduction

Nowadays, epoxy thermosetting resins present many application fields such as composites matrix, adhesives, coatings, and even polymer 3D-structures, due to their excellent mechanical and thermal properties. However, their main limitation lies in their low conformability, which clashes with the growing demand for complex shape designs. New processing technologies with higher design freedom, such as 3D-printing, are currently being developed. Several researchers [1–4] have proposed an interesting alternative strategy based on thermosets with sequential dual curing. Sequential dual-cured resins are synthesised through two compatible chemical curing reactions, which take place sequentially in a controlled way. This control can be carried out by combining two different stimulated polymerisation reactions, such as photothermal curing [5,6], or two thermal curing reactions with different activation temperatures. An interesting proposal of this last approach is the combination of thiol–epoxy reaction and epoxy homopolymerization [1,4]. The off-stoichiometric thiol–epoxy reaction occurs at a relatively low curing temperature, forming an intermediate and stable resin, which can be easily shaped and conformed due to its low stiffness. Then, the 3D complex design is fixed with a second thermal treatment for epoxy homopolymerisation, which occurs at a higher temperature catalysed by a latent catalyst.

Shape memory (SM) is another recent approach for enhancing the conformability of thermosetting resins, adopting several stable temporary shapes and recovering their original permanent one upon the action of an external stimulus [7]. The most developed SM resins require thermal stimuli. In fact, any thermoset can be thermally SM programmed, switching the shape and fixing processes at its glass transition temperature (Tg). At the rubbery stage, the shaping implies conformational rearrangements of chain segments between crosslinks. Therefore, the cooled temporary shape has stored strain energy as stressed material, which is entropically released when the permanent shape is restored by heating above Tg. Polymer networks with coexisting soft and rigid phases present enhanced SM efficiency. Numerous works are being published about the tailoring of epoxy network structures to enhance their SM performance. One of them is the combination of aliphatic and aromatic hardeners with different chain lengths [8,9] and even the breakage of the epoxy/amine stoichiometric ratio in order to tailor their viscoelastic properties: Tg and the glassy and rubbery storage modulus [10]. For the same reason, the off-stoichiometric dual epoxy resins also present SM [11], because their chemical structure is constituted by thiol–epoxy segments and stiffer epoxy homopolymerized chain segments.

In any case, the post-curing by homopolymerization or the recovery of the permanent shape requires a secondary thermal treatment, which significantly reduces the capability of in-situ post-processing and therefore their final application. The addition of graphitic or metal nanofillers at percentages higher than the electrical percolation threshold allows heating by the Joule effect by applying an electrical voltage [12,13]. In this way, the thermally activated processes become electrical triggering ones, broadening their feasibility. The thermoelectrical behaviour of materials is described by the following laws:

$$\text{Ohm's law:} \quad V = IR \tag{1}$$

$$\text{Joule's law:} \quad Q = V \cdot I \cdot t \tag{2}$$

where Q is the heat flow in a time t, V is the applied voltage, I is the transported current and R is the intrinsic electrical resistance of the system.

Therefore, the increase of temperature due to Joule heating can be calculated by:

$$\Delta T \propto \frac{V^2}{R} \tag{3}$$

This means that the most efficient electrical heating materials will be obtained by increasing their electrical conductivity or reducing the heated area between electrodes, in order to reduce the electrical resistance.

The addition of graphic nanofillers into epoxy resins to increase their electrical conductivity and to induce Joule heating has been studied to other authors [14–16] in order to activate thermal stimulated functionalities, such as shape memory. Instead of using external heating, a DC voltage is applied to the material, inducing a heating according Joule law and triggering shape recovery. Therefore, the resin become in electro-active materials, increasing their applicability. Moreover, the resistive heating is faster and requires low energy consumption [15]. In this application, SM resins can return to their pre-deformed shape by application of external stimuli. The traditional heating by convection requires the introduction of the specimen in an oven or the use of heating blanket. In any case, the heating requires heat flow from the surface to inside the material, which present low efficient due to the low thermal conductivity of the resins. Moreover, this heating could be not totally homogenous, generating internal thermal stresses and thermal gradients in large specimens, which could affect to the final recovery shape. The electrical stimulation is an inner heating from the graphitic nanofillers to the polymer matrix, being more efficient due to their high dispersion on the resin. The resistive treatment needs the application of a DC voltage, which only requires the need of electrodes over the sample surfaces and an electrical source. This justifies their easy implementation and in situ applicability.

In this work, a sequential dual thiol–epoxy system, previously optimised [1,2,4], was used as a matrix of nanocomposites doped with carbon nanotubes (CNTs). The epoxy conversion reached, the crosslinking density and ultimately the chemical structure formed during the first and second curing stages in the studied epoxy resins and nanocomposites were analysed by Fourier transform infrared spectroscopy (FTIR), differential scanning calorimetry (DSC) and a dynamic mechanical thermal analyser (DMTA). In addition, the thermal and thermo-mechanical properties were determined to evaluate the viscoelastic properties and therefore to establish the SM conditions. Next, the electrical and thermoelectrical behaviour of the nanocomposites was evaluated with an electrical source-meter and infrared camera to determine the

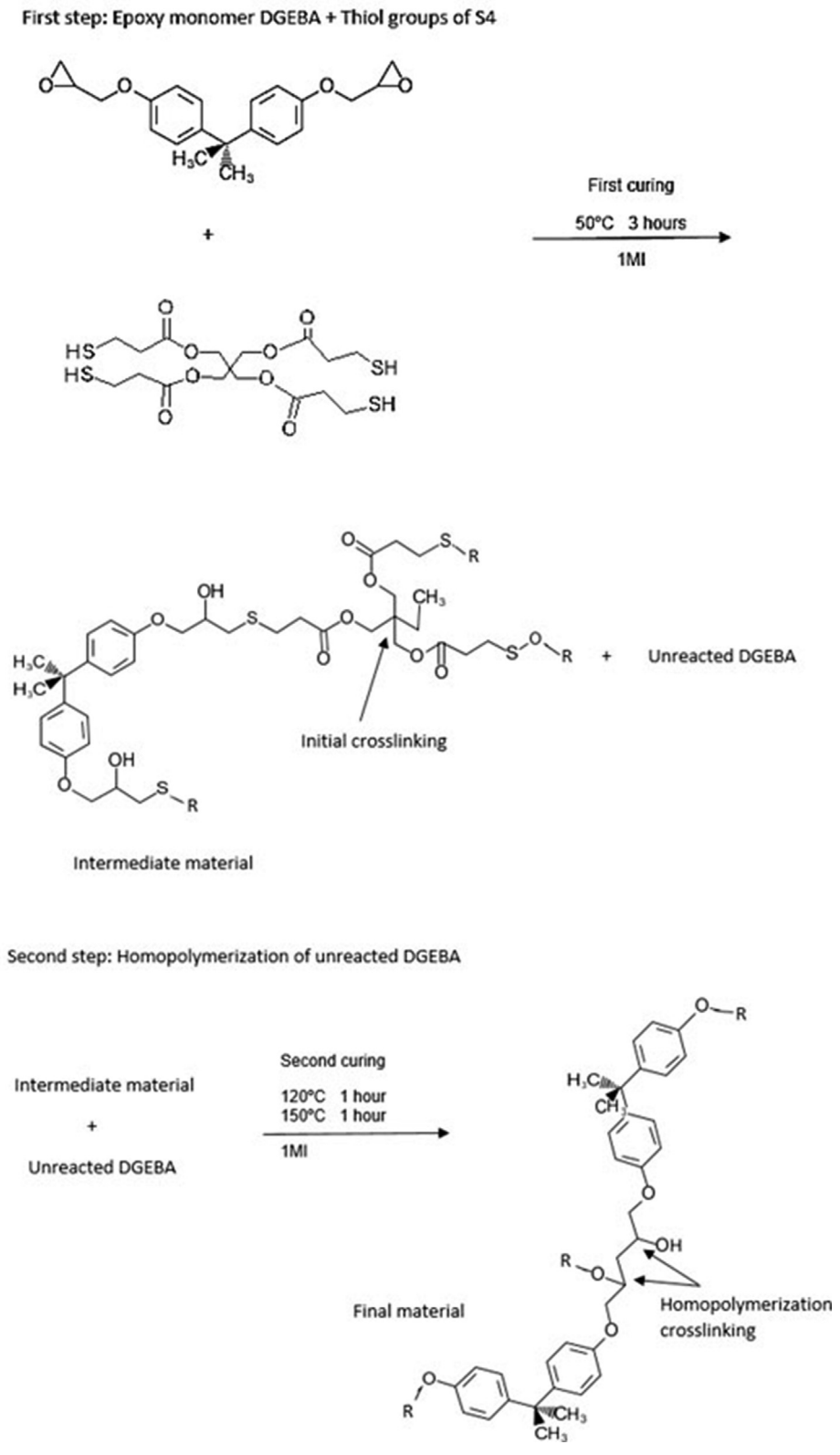

Fig. 1 – Chemical mechanism of the sequential dual curing process for the system DGEBA/S4/1MI.

electrical conductivity of the nanocomposites and the Joule heating capability as a function of the applied voltage. Finally, different U-type bending tests were applied to confirm the easy shaping and conforming of the studied dual-epoxy resins and the SM performance of the nanocomposites thermally triggered by traditional convection and Joule heating.

2. Materials and methodology

2.1. Materials

Epoxy monomer, diglycidyl ether of bisphenol A (DGEBA, Sigma Aldrich), with a molecular weight per epoxy equivalent of 170.2 g/eq was dried at 80 °C under vacuum for several hours prior to manufacture. Pentaeritritol tetrakis(3-mercaptopropionate) (S4, Sigma Aldrich) with a molecular weight per thiol equivalent unit of 122.17 g/eq was used as co-monomer of the first curing reaction, while the epoxy homopolymerisation, at higher curing temperature, was catalysed by 1-methylimidazole (1MI, Sigma–Aldrich). The dual-epoxy resin was doped with multi-walled CNTs (NC7000, Nanocyl), whose average diameter and length are 9.5 nm and 1.5 μm, respectively. Their specific surface is in the range of 250–300 m^2/g and their purity is higher than 90%. Their volumetric electrical conductivity, measured by the supplier, is 10^6 S/m.

Epoxy networks were manufactured with different thiol–epoxy ratios (0.6, 0.8 and 1) adding 1 wt% 1MI as catalyst. The applied curing process was carried out in two steps: the 1st curing stage at 50 °C for 3 h to ensure the full thiol/epoxy reaction and the 2nd curing stage at 120 °C for 1 h followed by 150 °C for 1 h, to ensure the complete homopolymerisation of the remaining epoxy groups.

Epoxy nanocomposites were manufactured by adding 0.2 wt% CNT, a percentage higher than the electrical percolation network. The dispersion of CNT into DGEBA was carried out with a three-roll mini-calander (Exakt 80E) at 40 °C, using a previously optimised dispersion procedure [14, 17].

2.2. Characterisation

The chemical structure of the networks was analysed by FTIR (Thermo-Nicolet Avatar 380) with and attenuated total reflectance (ATR) device. IR spectra were collected at 2 cm^{-1} in the range of 300–4000 cm^{-1} wavenumber.

The glass transition temperature and residual exothermal curing peak were determined by DSC (Mettler 822e), applying two consecutive dynamic scans, from −50 to 200 °C, at 10 °C/min, following the standard ASTM E1356.

The morphology of nanocomposites was analyzed by field emission gun scanning electron microscopy (FEG-SEM) and transmission electron microscopy (TEM). The samples were cut by previous immersion in liquid nitrogen to avoid the fractography. The cryogenic fracture enhances the observation of morphology to evaluate the dispersion of carbon nanotubes. Then, the surface were coated with a thin layer (2 nm) of Pt for FEG-SEM observation. The experimental conditions of sputtering were 30 mA for 120 s (Bal-tec, SCD-005 sputter).

DMTA, using a DMA Q800 V7.1 analyser from TA Instruments, was used to evaluate the thermomechanical behaviour and viscoelastic properties of the studied samples. The samples (12.5 × 1.5 × 35 mm^3) were tested in single cantilever mode, at 1 Hz, from room temperature (RT) to 200 °C, with a heating rate of 2 °C/min. From the statistical theory of rubber elasticity [11], the crosslinking density (υ_c) can be calculated by:

$$\upsilon_c = \frac{E'_R}{3RT} \quad (4)$$

where E'_R is the storage modulus in the rubbery state at temperature T, which is Tg + 30 K (the Tg measured as the maximum of tan δ), while R is the gas constant.

Electrical conductivity was measured by an electrical current source meter (Keithley 2410), according to ASTM D4496. The contacts over the samples were silver-pasted to minimise the contact resistance between the sample, and copper wires were used as electrodes. The specimens (10 × 10 × 1 mm^3)

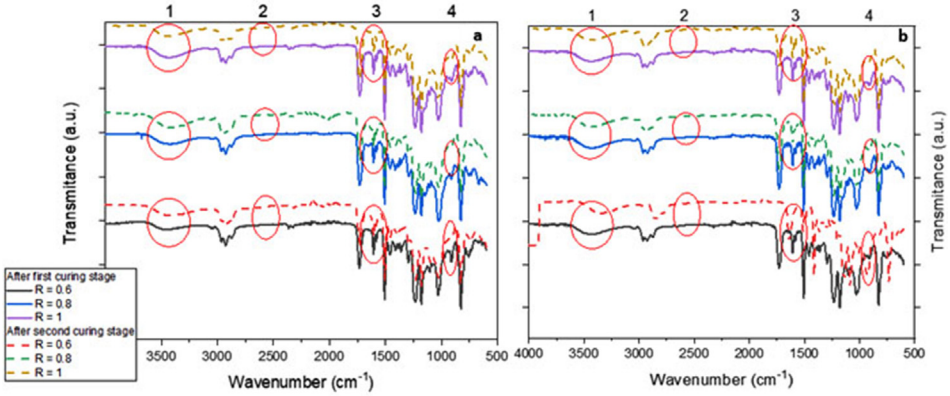

Fig. 2 – FTIR spectra of cured nanocomposites doped with 0.2 wt% with different thiol–epoxy ratios (R = 0.6, 0.8 and 1.0) and 1 wt% 1MI, before and after the second curing stage at high temperature for neat resins (a) and nanocomposites reinforced with 0.2 wt% CNT (b). The circled bands correspond to 1) hydroxyl, 2) thiol, 3) aromatic C–C, and 4) oxirane rings.

were tested from 0 to 50 V, collecting the transported current, with a compliance of 20 mA for 60,000 ms.

Joule heating was measured using a thermal camera (FLIR E50) coupled and synchronised up to a current source meter (Keithley 2410). Different constant voltages, from 10 to 90 V, were applied over the samples (12.5 × 1.5 × 35 mm^3), determining the average and the maximum temperature reached, starting at 21 °C.

Finally, the shaping and SM ability were determined by a U-type test [15, 18], using two different moulds to fix the temporary shape, with angles of 45° and 90°, which correspond with 76 and 38 mm of curvature radius, respectively. Rectangular bar specimens (13 × 2 × 80 mm^3) were heated and deformed to a U shape in a specific mould (θ_{max}) applying a constant force. The deformed sample was rapidly cooled down to RT to fix the temporary shape (θ_{fixed}). Then, the sample was again heated up to the transition temperature to induce the recovery of the permanent shape (θ_{rec}). In order to quantify the behaviour, the shape fixing (S_F) and recovery (S_R) ratios were calculated by the following equations:

$$S_F(\%) = \left(\frac{\theta_{fixed}}{\theta_{max}}\right) \times 100 \quad (5)$$

$$S_R(\%) = \left(\frac{\theta_{rec}}{\theta_{max}}\right) \times 100 \quad (6)$$

The measurements of angles were carried out by image analysis using Image J software.

3. Results and discussion

Fig. 1 shows a schematic illustration of the proposed sequential dual curing process. First, at low temperature, the oxirane rings of the epoxy monomer (DGEBA) react with thiol groups of hardener (S4). The reaction occurs up to the most of thiol groups have reacted. Then, in the second curing stage, the homopolymerization occurs between the excess oxirane rings at high temperature. This postcuring reaction is activated by the imidazole catalyser.

Fig. 2 shows the FTIR spectra of the neat resins and composites. Each sample is analysed before and after the second curing stage, in order to determine the chemical structure developed in the first curing stage due to the thiol–epoxy reaction at low temperature and the final crosslinked network, completed by epoxy homopolymerization at higher temperature. Neat epoxy resins and nanocomposites doped with 0.2% CNT were synthesised with different thiol–epoxy ratios (R = 0.6, 0.8 and 1.0). Lower ratios were not analysed due to drop formation during forming, as observed previously by other authors [2], consisting in a significant dripping of the samples during the second stage, hindering their shaping.

The circled IR bands correspond to stretching [1] of C–O–C oxirane rings at 915 cm^{-1}; C=C aromatic rings at 1605 cm^{-1} (used as the reference band); S–H at 2560 cm^{-1} and O–H around 3500 cm^{-1}. According to the chemical reactions, in the first curing stage, at the maximum conversion, the thiol band must disappear while the epoxy band must reduce its intensity as a function of the thiol–epoxy ratio of the sample. In any case, an increment of hydroxyl groups must be registered. The second curing reaction is followed by the disappearance of oxirane and the increase of hydroxyl bands.

The thiol band had disappeared for all the studied samples, epoxy resins and nanocomposites doped with CNT, with different thiol–epoxy ratios, after the first curing treatment, indicating the total conversion. The increment of epoxy conversion during the second curing stage is calculated from the normalised absorbance of the epoxy band before and after this thermal treatment:

$$\Delta\alpha_e = \frac{\left(\frac{A^2_{915}}{A^2_{1605}}\right) - \left(\frac{A^1_{915}}{A^1_{1605}}\right)}{\left(\frac{A^1_{915}}{A^1_{1605}}\right)} \quad (7)$$

The subscript indicates the IR band, at 915 cm^{-1} for epoxy groups and at 1605 cm^{-1} for aromatic C–C, used as reference. The superscript indicates the thermal curing treatment applied, 1 after the first and 2 after the second curing stage.

Table 1 collects the increment of epoxy conversion for the second curing stage. As expected, for neat epoxy resins, the breakage of the thiol–epoxy ratio enhances the epoxy homopolymerization in the second curing stage. However, unexpected results are obtained for the nanocomposites doped with 0.2 wt% CNT. The second thermal treatment has no influence on the epoxy conversion. This could be explained by two different phenomena: 1) CNTs act as catalyst of the epoxy homopolymerization reaction, which occurs at the same time as the thiol–epoxy reaction, at low temperature, 50 °C or, on the contrary, 2) CNTs absorb or react with 1MI molecules, inhibiting the subsequent homopolymerization. The near-disappearance of the epoxy IR band, at 915 cm^{-1}, during the first curing stage of off-stoichiometric CNT/epoxy nanocomposites, seems to indicate the occurrence of a secondary chemical reaction at low temperature. In order to confirm the effect of CNTs on the homopolymerization, a calorimetric study was carried out [19].

Fig. 3 shows some thermograms and the results obtained by DSC. The DSC thermograms for off-stoichiometric epoxy resins cured at low temperature (Fig. 3a) show the glass transition temperature of the thiol–epoxy network and then the exothermic peak corresponding to epoxy homopolymerization catalysed by 1MI. This peak is shifted at higher temperature when the thiol–epoxy ratio increases due to the lower concentration of the remaining oxirane groups. The stoichiometric sample, R = 1, reaches the maximum conversion within the first curing stage. However, no exothermic peak appears in the DSC thermograms collected for the CNT nanocomposites (Fig. 3b), confirming the IR results.

Table 1 – Increment of epoxy conversion on the second curing stage measured by FTIR ($\Delta\alpha_E$).

CNT	R	$\Delta\alpha_E$
0%	0.6	0.32
	0.8	0.28
	1.0	0.01
0.2%	0.6	0.04
	0.8	0.01
	1.0	0

Fig. 3c and d shows the Tg measured by DSC for each sample studied after the first and second curing stages, respectively. Fully homopolymerized samples (R = 0) are also included. The Tg measured for all the stoichiometric thiol–epoxy samples (R = 1) is very similar, close to 50 °C, indicating that the first curing stage, at 50 °C for 3 h is enough to reach the maximum conversion [2] for both neat and CNT doped resins. The maximum thiol–epoxy conversion is also reached for all the studied samples, regardless of the stoichiometric ratio and CNT addition, during the first curing stage. On the contrary, significant differences are observed in the Tg measured after the second curing stage. Neat epoxy resins follow the expected behaviour [D, E, H], increasing the Tg of the network due to the epoxy homopolymerization catalysed by 1MI, which occurs at high temperature. Tg increases proportionally with the percentage of the homopolymerized epoxy chain segments due to their highly dense crosslinking. In fact, the Tg values of the stoichiometric samples are 50 and 140 °C for thiol–epoxy resin (R = 1) and totally homopolymerized resin (R = 0), respectively. The off-stoichiometric epoxy networks (R 0.6 and 0.8) present intermediate values. Again, the second curing stage allows the maximum epoxy conversion to be reached, getting the maximum Tg of the cured network.

Very striking results are obtained for CNT/epoxy nanocomposites. Tg reached during the first curing stage is higher than the measured ones for neat epoxy resins. However, the second curing stage and the dynamic second DSC scan of the nanocomposites only provide a slight increment on the Tg, confirming that the exothermic homopolymerisation reaction does not occur at higher temperatures, but during the first thiol–epoxy step.

It is worthy to note that in the second DSC scans, the Tg of neat stoichiometric epoxy resin (R = 1) reaches 120 °C after curing at 50 °C and postcuring at 150 °C (Fig. 3d) and close to 140 °C for the sample cured only with the fist treatment, at 50 °C (Fig. 3c). This behaviour is justified because the dynamic thermal postcuring is more efficient than the isothermal curing and postcuring treatment, allowing reaching higher conversion degree of the network.

In fact, it is worth noting that the Tg of the neat DGEBA/1MI mixture (R = 1) reaches 140 °C while it is reduced to 90 °C for the same homopolymerized nanocomposites doped with 0.2 wt% CNT. This effect was not observed previously in the bibliography.

Numerous papers have been published about the effect of carbon nanotubes on the curing reaction of epoxy resins [21–24], especially when the graphitic nanofillers are chemically functionalised [25]. In fact, controversial results have been published indicating that the graphitic nanofillers can act as catalysts [20,23] or, contradictorily, they can inhibit, retard or hinder the curing reaction [24]. This anomaly could be associated with the different dispersion degree of the nanocomposites, since isolated nanotubes and agglomerates

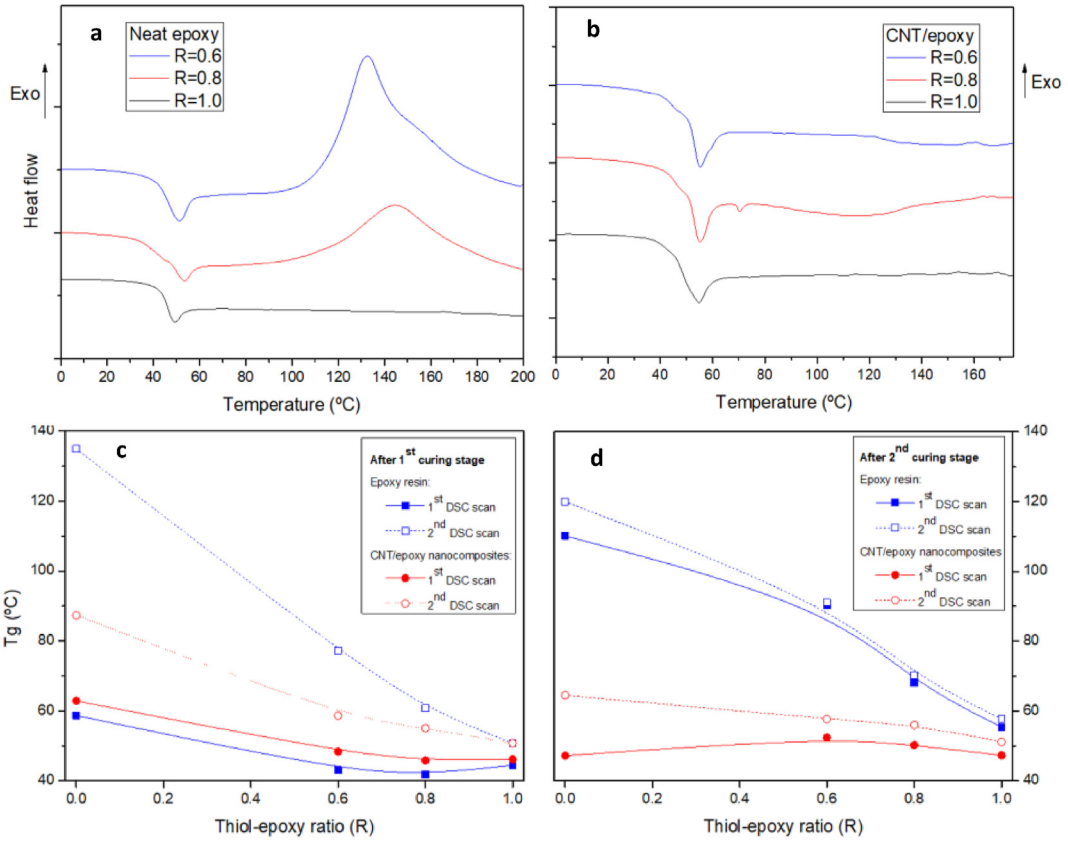

Fig. 3 – DSC thermograms of epoxy resins (a) and CNT/epoxy nanocomposites (b) with different thiol–epoxy ratios (R) cured with the first curing stage at low temperature. Glass transition temperature measured by DSC of the samples cured at low temperature with first curing stage (c) and samples totally cured after second curing stage (d).

lead to different effects. Most of them agree that the addition of multi-walled carbon nanotubes [20,24] induces a decrease of the reaction temperature due to the increase of the gel activation energy in comparison with that of the neat epoxy resin. Moreover, our experimental results obtained confirm that CNTs hinder or inhibit the homopolymerization reaction during the postcuring process, where the reaction is controlled by diffusion due to the devitrification of the system when the temperature reaches the Tg value of the system. Therefore, the CNT effect on the postcuring reaction must be associated with an inhibition effect of the imidazole catalyser, as it will be explained below.

Zhou et al. [24,26] studied the effect of non-functionalised multi-walled carbon nanotubes on the curing reaction of epoxy resin cured with imidazole hardener (2-ethyl-4methylimidazole, EMI). They drew the same conclusions as those observed for the epoxy curing reaction with amine hardeners [20], but the effect seemed to be more acute. CNTs act as catalyst, facilitating the curing and accelerating it. The accelerating effect is noticeable at low CNT contents (<1 wt%), reaching a saturation at higher percentages. This catalytic behaviour has a positive effect, shortening the pre-curing time and decreasing the pre-curing temperature. However, CNTs also have a negative effect due to hindering the vitrification phenomenon. CNTs prevent the occurrence of vitrification, needing a longer post-curing time and higher post-curing temperature. In these systems, the autocatalytic mechanism is not modified but the overall degree of curing decreases with the presence of CNTs, as evidenced by the lower total reaction heat and the lower Tg of cured composites compared with neat epoxy resins.

On the other hand, Chen et al. [27] published a study about homopolymerized epoxy nanocomposites doped with multi-walled CNT, in which no clear differences were observed between the curing reaction of the neat epoxy resins and nanocomposites. The epoxy curing reaction was an anionic homopolymerization initiated by a tertiary aromatic amine, 4-dimethylamino pyridine (DMAP). This confirms that the unexpected behaviour of our studied system is not explained by the anionic homopolymerization. Therefore, it is associated with the interaction between CNTs, used as nanofillers, and 1-methylimidazole, used as catalyst.

It is worth noting that the CNTs used are non-functionalised, for which reason the observed catalytic effect cannot be associated with the presence of hydroxyl groups or other polar functional groups. The phenomenon must be associated with the conjugated aromatic C–C structure of the carbon nanotubes.

Imidazole can be anchored by π–π interactions over the conjugated C–C structure of the nanotubes. Some studies [28–30] confirm that this non-covalent interaction is relatively weak with molecules containing single benzene rings, such as styrene. Conjugated C–C structures containing substituents, such as amino or cyano, can absorb electrons or supply electrons, changing the electron cloud density of the molecule, and allowing donor–acceptor interaction with carbon nanotubes, which enhances the π–π anchoring. In this case, the imidazole interacts with the carbon nanotubes by π–π interactions strengthened by electron donor–acceptor interaction. This does not provide the degradation of the imidazole structure, but the results obtained confirm that its reactivity is altered.

The π–π anchoring of imidazole over carbon nanotubes seems to enhance their catalytic efficiency, decreasing the homopolymerisation curing temperature. However, this also causes the reduction of their mobility and diffusion ability at low temperature. This could explain the higher Tg reached by the CNT/epoxy nanocomposites with thiol–epoxy ratios of 0, 0.6 and 0.8, after the first curing stage, at low temperature, and the lower Tg after the second curing stage, at high temperature, regarding neat epoxy resins. This explanation is in agreement with previous results published [24,26] using EMI as the curing agent. However, the catalytic effect on our system, where imidazole is used as the catalyst/initiator, seems more marked due to the low imidazole concentration added.

In order to confirm this, the crosslinking density is determined by DMTA results from the rubbery storage modulus (Eq. (4)). Fig. 4 shows the crosslinking density as a function of the thiol–epoxy ratio for neat epoxy resins and nanocomposites after first and second curing stages. As expected, the lowest crosslinking density is obtained for off-stoichiometric neat epoxy resins after the first curing treatment at low temperature because these networks are only formed by the reaction of thiol groups with 60% and 80% of the epoxy groups from DGEBA. However, the crosslinking density of stoichiometric epoxy resin (R = 1) is high and is scarcely modified during the second curing stage, indicating again that the maximum thiol–epoxy conversion is reached at low temperature. In contrast, the off-stoichiometric epoxy networks are strongly crosslinked during the second curing treatment at high temperature due to the epoxy homopolymerization catalysed by imidazole.

The crosslinking density of CNT/epoxy nanocomposites is clearly different from those measured for neat epoxy resins. The initial networks for off-stoichiometric nanocomposites formed during the first curing stage reach a relatively high degree of crosslinking due to the occurrence of two curing

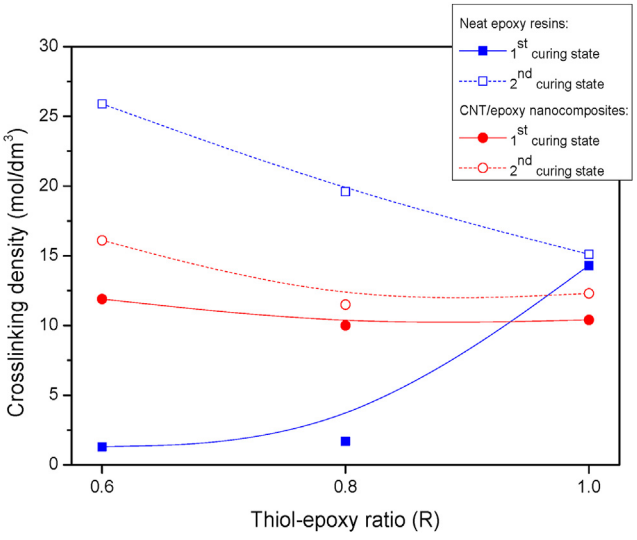

Fig. 4 – Crosslinking density of epoxy resins and CNT/epoxy nanocomposites with different thiol–epoxy ratios, after the first and second curing stages.

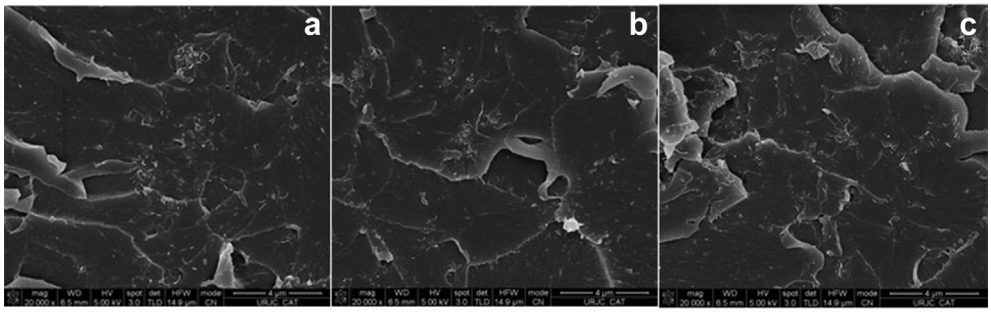

Fig. 5 – FEG-SEM micrographs of the nanocomposites doped with 0.2 wt% CNT with different thiol–epoxy ratio: 0.6 (a), 0.8 (b) and 1.0 (c).

reactions: thiol–epoxy and epoxy–epoxy homopolymerization. However, the second curing process at high temperature scarcely affects the degree of crosslinking. The crosslinking density of a totally cured network for off-stoichiometric neat epoxy resins is much higher than that reached for CNT/epoxy nanocomposites, indicating that in the case of neat epoxy resins the sequential curing reactions are more effective. First, the thiol–epoxy reaction occurs at low temperature, and then homopolymerization takes place at high temperature. For CNT/epoxy nanocomposites, both competitive reactions occur simultaneously, decreasing the degree of crosslinking of the final networks.

Fig. 5 shows some images obtained by FEG-SEM, which allows us observing the morphology of the nanocomposites in order to evaluate the dispersion degree of the CNTs into the matrix. A relative good dispersion is observed. They are well distributed in the epoxy resin although some small agglomerates can be still observed. The size of these CNT aggregates are smaller than 500 nm, indicating a suitable dispersion. No differences are observed as a function of the thiol–epoxy ratio. This was expected because the dispersion process is carried out on the DGEBA/CNT mixture. The curing crosslinking degree does not affect to CNT distribution. It is worthy to note that the morphology of the fracture is similar due to the cryogenic fracture. For this reason, substantially differences on the fracture surfaces are not observed either.

Table 2 – Thermomechanical properties determined by DMTA: storage modulus at glassy (E'_G) and glass transition temperature (Tg) measured by the maximum of tan δ peak, for epoxy resins and CNT/epoxy nanocomposites with different thiol–epoxy ratios, after first and second curing stages.

CNT	R	E'_G (GPa)		Tg (°C)	
		1st curing stage	2nd curing stage	1st curing stage	2nd curing stage
0%	0.6	1.2 ± 0.6	2.0 ± 0.6	50.0 ± 0.5	108.9 ± 1.7
	0.8	2.1 ± 0.5	3.1 ± 0.9	65.6 ± 1.7	72.9 ± 2.3
	1.0	2.0 ± 0.3	2.0 ± 0.4	60.4 ± 1.2	61.8 ± 2.1
0.2%	0.6	2.5 ± 0.1	2.6 ± 0.3	63.3 ± 0.2	67.1 ± 0.5
	0.8	2.6 ± 0.2	2.6 ± 0.4	62.7 ± 1.1	65.5 ± 1.0
	1.0	2.2 ± 0.2	2.5 ± 0.3	58.5 ± 1.1	60.5 ± 0.8

The DMTA results obtained are collected in Table 2. The Tg values measured as the maximum of the tan δ peak by DMTA follow the same behaviour as the DSC results. The relaxation temperature is low for neat epoxy resins after the first curing stage due to the thiol–epoxy reaction and significantly increases for the second curing stage at high temperature due to homopolymerization. This Tg increment is higher as the thiol–epoxy ratio decreases due to the high percentage of densely crosslinked homopolymerized chain segments. In contrast, the glass transition of epoxy nanocomposites remains practically constant regardless of the thiol–epoxy ratio and curing stage applied. As explained before, in these nanoreinforced samples, both the thiol–epoxy and epoxy–epoxy reactions occur simultaneously at low temperature, decreasing the maximum degree of crosslinking reached due to the lower efficiency in comparison with the sequential reactions that occur with neat epoxy resins.

The stiffness of off-stoichiometric epoxy resins significantly increases during the second curing stage, while this property remains constant for neat stoichiometric epoxy resin, due to the homopolymerisation at high temperatures of non-stoichiometric samples. The samples after first stage has a modulus between 1.2 and 2.1 GPa, being lower for the samples with lowest amount of S4, due to they are the resins with lowest crosslinking degree. After second stage, the modulus is approximately constant for all the neat samples due to all reached the maximum crosslinking degree. The neat resins, after second thermal treatment, present a modulus similar to traditional epoxy-amine resins, in the range of 2–3 GPa, which confirms their applicability, taking into account their easy thermal conforming before the second curing treatment. Fernandez-Francos et al. [1], Belmonte et al. [2,3] and Konuray et al. [4] have published a deeper characterization of this neat system, confirming the same conclusions.

It is worthy to note that in spite of the lower crosslinking density of CNT/epoxy networks due to the inhibition of homopolymerization, these samples are stiffer due to the reinforcement effect of CNTs. The storage modulus remains constant for all studied reinforced samples with any influence of the stoichiometry and curing treatment applied.

Once the main chemical structure of the studied resins and nanocomposites was known, the shaping and shape memory behaviour were analysed. All the experiments were

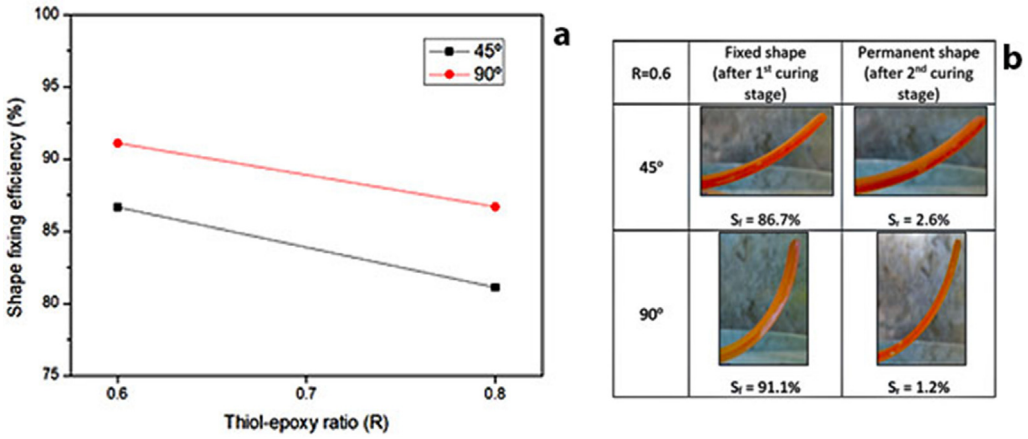

Fig. 6 – Shape fixing efficiency at 60 °C of off-stoichiometric resins cured with the first curing stage (a), and photographs and values of shape fixing efficiencies for the resin with a thiol–epoxy ratio of 0.6 (b).

performed using two U-type moulds with 45° and 90°, corresponding to 76 and 38 mm of curvature radius. The shape fixing and recovery efficiency were calculated using Eqs. (5) and (6), respectively.

Shaping and forming at low temperature were carried out for neat off-stoichiometric resins before the second curing stage. The shaping temperature was 60 °C, higher than the Tg reached during the first curing, 50.0 and 65.5 °C for the samples with R = 0.6 and 0.8, respectively. It is required that the samples are softened to be bended but the temperature cannot be so high in order to avoid the postcuring reaction by homopolymerization. Fig. 6a shows the shape fixing efficiency, being in the range of 80–90%. The decrease of the thiol–epoxy ratio enhances the thermo-conforming process of the epoxy resins due to the lower degree of crosslinking reached for the first curing stage. In addition, the higher deformation enhances the shaping efficiency. On the other hand, the shape recovery performance is good for thermoforming process of thermosets. The studied off-stoichiometric epoxy resins have a sequential dual-curing process, allowing their shaping and forming at relatively low temperature. Then, the shape is fixed for the second curing stage (Fig. 6b), obtaining complex geometries of highly crosslinked epoxy resins, which are not available for conventional thermosets.

Moreover, the studied epoxy resins and composites present SM behaviour. SM is based on the relaxation of thiol–epoxy chain segments at low temperature, while the homopolymerized segments between crosslinking points remain unaltered. For this reason, the SM triggering temperature of totally cured epoxy resins and nanocomposites is above the Tg measured before the second curing stage. In this case, the SM triggering temperature applied was 70 °C. Both the shape fixing and recovery efficiencies measured were in the range of 60–80% for all the studied samples. No greater differences are observed for all the studied samples. Only, as expected, the SM efficiency of less stiff samples, with low thiol–epoxy stoichiometry, and non-doped ones, was

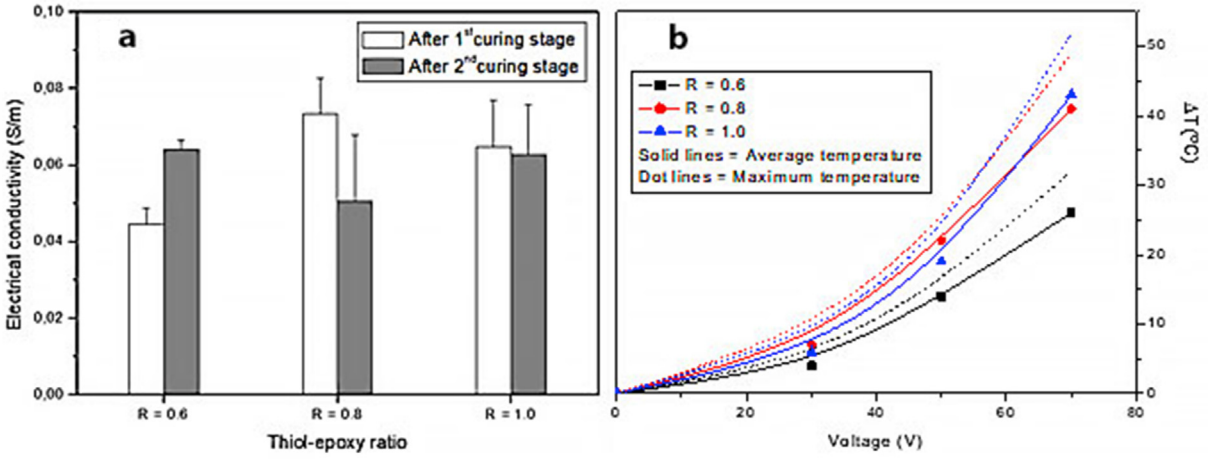

Fig. 7 – Electrical conductivity (a) for epoxy nanocomposites with different thiol-epoxy ratios after first and second curing stage and increment of temperature due to Joule-s heating (b) after second curing stage.

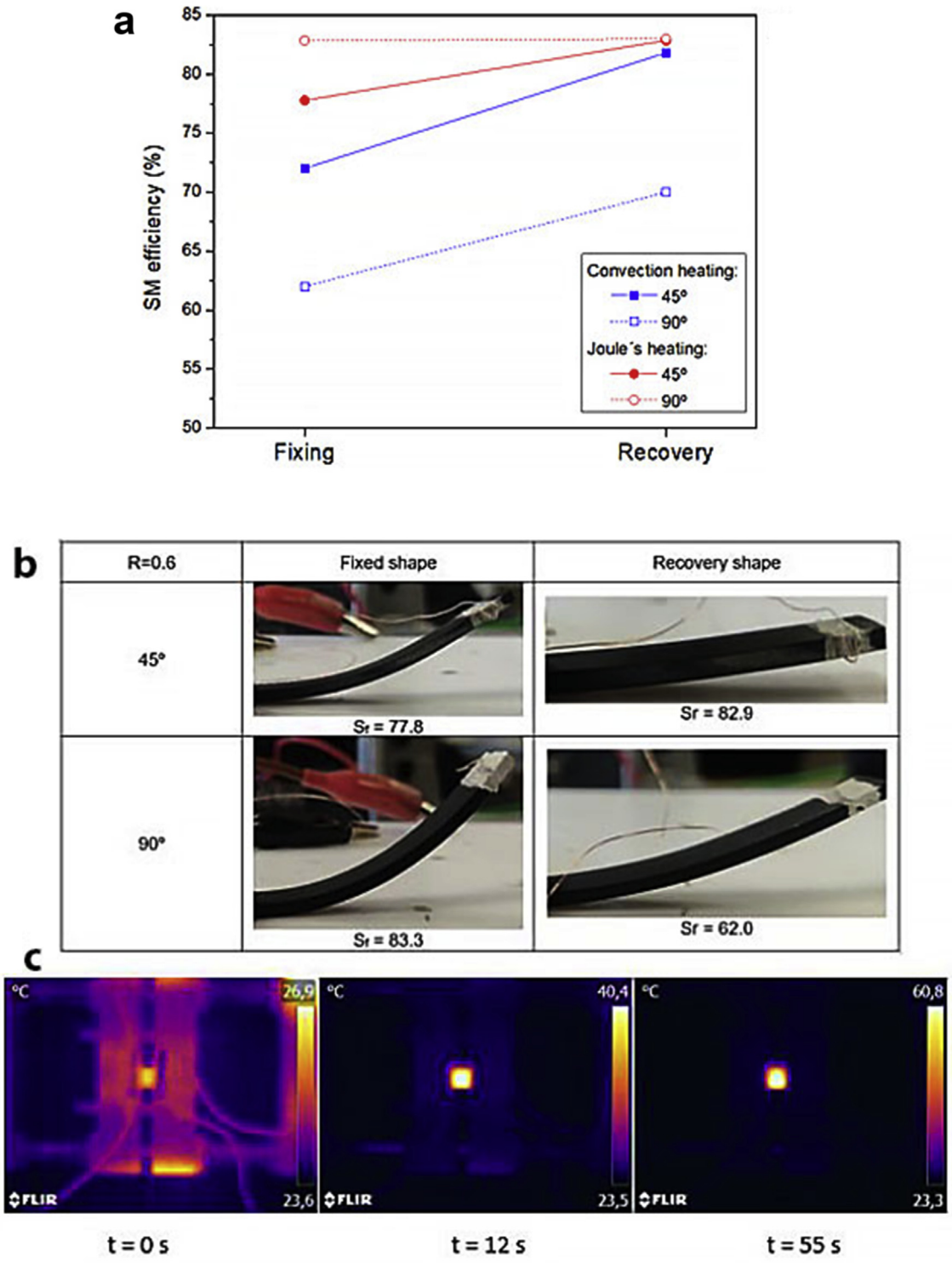

Fig. 8 – Shape fixing and recovery efficiency of CNT/epoxy nanocomposites with a thiol-epoxy ratio of 0.6 by convection heating in oven and Joule's heating (a), photographs and values of fixed shape and recovery shaped for CNT/epoxy nanocomposite with a thiol–epoxy ratio of 0.6 (b), and Joule's heating for same sample (c).

relatively higher. This behaviour was previously studied in depth by other authors [2,3].

The aim of adding CNTs is to increase the electrical conductivity of insulating resins due to the formation of electrically percolated CNT networks. The electrical conductivity of the studied nanocomposites is shown in Fig. 5a. All the nanocomposites followed Ohm's law (Eq. (1)), showing a linear relationship between the electrical current and the applied voltage. The electrical conductivity of the nanocomposites is in the range of 0.4–0.6 S/m, without any differences between

them, as a function of the stoichiometric ratio or the curing treatment applied. This means that the degree of crosslinking of the epoxy matrix scarcely affects the electrical conductivity of the nanocomposites. In addition, it is confirmed that the electrical percolation threshold of the studied system is lower than 0.2 wt% CNT. Due to the relatively high electrical resistivity of the nanocomposites, the application of an electrical voltage induces a heating due to the Joule effect (Eqs. (2) and (3)), which is shown in Fig. 7b. The application of relative low electrical voltage, < 80 V, induces the heating of the nanocomposites up to temperatures in the range of 20–50 °C. In spite of the similar electrical conductivity, Joule's heating seems to be more efficient for the nanocomposites high thiol-epoxy ratio, which are the samples with high crosslinking degree. As it was previously confirmed the imidazole catalyser reacts with CNTs, inhibiting the homopolymerization for the nanocomposites with thiol-epoxy ratio of 0.6 and 0.8%. This interaction seems to lead a negative effect on the Joule heating. Resistive heating for the nanocomposite with a thiol-epoxy ratio of 0.6% is hindered, which could be explained by differences of the thermal conductivity of the system.

In this context, the thermoelectrical behaviour of nanocomposites can be useful in order to convert the thermally stimulated shape memory into an electrically switched one, significantly enhancing their applicability. Fig. 8 shows a comparison of the SM fixing and recovery efficiencies using two different energy sources: conventional heating in an oven and thermoelectrical heating by the Joule effect, up to 70 °C.

It is clearly observed that the SM efficiency for both processes, fixing and recovery, is more effective for Joule heating because it is an intrinsic heating. Moreover, Joule heating is much faster, requiring fixing times of 3–5 min, but the recovery time is lower than 30 s. Previous published works have confirmed the higher shape fixing and recovery rates [14–16] by resistive heating. While the heating in an oven is from the surface to inside, Joule heating is caused by the heating of the electrical fillers into the matrix. Moreover, it is well known that the electro-resistive heating is very fast. However, the higher SM efficiency for Joule heating must be associated with a lack of time for heating in oven, in spite of that the samples were heated during 15 min. Therefore, the main conclusion of these results is that the SM rates is at least four time faster by Joule effect than conventional heating, in addition to be localized, because it is not required the heating of the entire sample, and their easier industrial implementation.

In all cases, the shape fixing efficiency is lower than the recovery efficiency due to the high stiffness of nanocomposites. During fixing of the temporary shape, the chain segments adapt to the external load by conformational rearrangements, storing strain energy. The strain energy stored in this way is released when the nanocomposite is unloaded and heated, restoring the permanent shape. For this reason, the shape fixing of epoxy resins is generally higher than that measured for nanocomposites. This is explained by the fact that epoxy resins have higher free volume and free movement between crosslinking points than nanocomposites. However, the shape recovery depends on the ability to remove the storage energy from the stressed samples, this being higher for nanocomposites. Therefore, the shape recovery efficiency depends on shape fixing.

Conventional heating in an oven by heat convection is slow. For this reason, in spite of the long fixing time applied (30 min), the fixing efficiency decreases significantly with the angle of deformation. Higher fixing times could avoid this problem. On the other hand, the fixing efficiency for the fast Joule heating is scarcely affected by the degree of strain.

In summary, in addition to its high applicability, Joule heating for the SM process is faster and more efficient than conventional heating.

4. Conclusions

Off-stoichiometric thiol–epoxy resins present sequential dual curing, enhancing their shaping and thermoconforming at low temperature before the second curing stage at high temperature. These systems cure at low temperature, around 50 °C, due to the thiol–epoxy reaction, reaching the maximum epoxy conversion. In this stage, the samples are easily formed at low temperature. Then, the complex geometry is fixed in a second curing stage at high temperature, inducing the homopolymerisation of the epoxy, catalysed by 1-methylimidazole.

The addition of carbon nanotubes (CNTs) significantly speeds up the homopolymerisation reaction, both chemical reactions occurring simultaneously. The final network of one-step cured nanocomposites at low temperature presents a lower crosslinking density than those developed by sequential dual curing of neat epoxy resins. CNT catalysis can be explained by the π–π anchoring of 1-methylimidazole over the carbon sidewalls of the nanotubes, enhanced by donor–acceptor interaction.

Off-stoichiometric epoxy resins and composites present shape-memory (SM) behaviour with high shape fixing and recovery efficiencies at a relatively low temperature, 70 °C, due to the relaxation of thiol–epoxy chain segments. The homopolymerised segments are steady at this temperature, which provides the advantage that the material maintains part of his mechanical properties during the SM processes, avoiding the need to use additional supports.

Nanocomposites can be SM-switched by the application of a low electrical voltage, inducing Joule heating. In addition to higher in-situ applicability, electrical resistive heating was probed to be faster, localized and more homogeneous than conventional heating in a convection oven. Therefore, the SM processes can be remotely activated quickly and very efficiently in this material, providing a very important advantage in locations with difficult access.

Funding

This work was supported by the Ministerio de Economía y Competitividad of Spain Government [PID2019-106703RB-I00]; and Comunidad de Madrid Government from Spain [ADITI-MAT-CM S2018/NMT-4411].

Declaration of Competing Interest

The authors declare that they have no known competing financial interests or personal relationships that could have appeared to influence the work reported in this paper.

REFERENCES

[1] Fernández-Francos X, Konuray AO, Belmonte A, De la Flor S, Serra A, Ramis X. Sequential curing of off-stoichiometric thiol-epoxy thermosets with a custom-tailored structure. Polym Chem 2016;7:2280–90.

[2] Belmonte A, Fernández-Francos X, Serra A, De la Flor S. Phenomenological characterization of sequential dual-curing of off-stoichiometric "thiol-epoxy" systems: towards applicability. Mater Des 2017;113:116–27.

[3] Belmonte A, Russo C, Ambrogi V, Fernández-Francos X, De la Flor S. Epoxy-based shape-memory actuators obtained via dual-curing off-stoichiometric "thiol-epoxy" mixtures. Polymers 2017;9:113.

[4] Konuray O, Arenya N, Morancho JM, Fernández-Francos X, Serra A, Ramis X. Preparation and characterization of dual-curable off-stoichiometric amine-epoxy thermosets with latent reactivity. Polymer 2018;146:42–52.

[5] Retailleau M, Ibrahim A, Allonas X. Dual-cure photochemical/thermal polymerization of acrylates: a photoassisted process at low light intensity. Polym Chem 2014;5:6503.

[6] Park YJ, Lim DH, Kim HJ, Park DS, Sung IK. UV- and thermal-curing behaviours of dual-curable adhesives based on epoxy acrylate oligomers. Int J Adhes Adhes 2009;29:710–7.

[7] Karger-Kocsis J, Kéki S. Review of progress in shape memory epoxies and their composites. Polymers 2018;10:34.

[8] Rousseau IA, Xie T. Shape memory epoxy: composition, structure, properties and shape memory performances. J Mater Chem 2010;20:3431–41.

[9] Liu Y, Han C, Tan H, Du X. Thermal, mechanical and shape memory properties of shape memory epoxy resin. Mater Sci Eng 2010;527:2510–4.

[10] Song W, Wang LY, Wang Z. Synthesis and thermomechanical research of shape memory epoxy systems. Mater Sci Eng 2011;529:29–34.

[11] Flory PJ. Molecular theory of rubber elasticity. Polymer 1979;20:1317–20.

[12] Orellana J, Moreno-Villoslada I, Bose RK, Picchioni F, Flores ME, Araya-Hermosilla R. Self-healing polymer nanocomposite materials by Joule effect. Polymers 2021;13(4):649.

[13] Prolongo SG, Moriche R, Del Rosario G, Jiménez-Suárez A, Prolongo MG, Ureña A. Joule effect self-heating of epoxy composites reinforced with graphitic nanofillers. J Polym Res 2016;23:189.

[14] Luo X, Mather PT. Conductive shape memory nanocomposites for high speed electrical actuation. Soft Matter 2010;6:2146–9.

[15] Zhou J, Li H, Liu W, Dugnani R, Tian R, Xue W, et al. A facile method to fabricate polyurethane based graphene foams/epoxy/carbon nanotubes composite for electro-active shape memory application. Compos Part A Appl Sci Manuf 2016;91(1):292–300.

[16] Wang W, Liu D, Liu Y, Leng J, Bhattacharyya D. Electrical actuation properties of reduced graphene oxide paper/epoxy-based shape memory composites. Compos Sci Technol 2015;106(16):20–4.

[17] Moriche R, Prolongo SG, Sánchez M, Jiménez-Suárez A, Sayagués MJ, Ureña A. Morphological changes on graphene nanoplatelets induced during dispersion into an epoxy resin by different methods. Compos B Eng 2015;72:199–205.

[18] Revathi KA, Rao S, Srihari S, Dayananda GN. Characterization of shape memory behaviour of CTBN-epoxy resin. J Polym Res 2012;19:9894.

[19] Chen JS, Ober CK, Poliks MD, Zhang Y, Wiesner U, Cohen C. Controlled degradation of epoxy network: analysis of crosslinking and glass transition temperature changes in thermally reworkable thermosets. Polymer 2004;45:1939–50.

[20] Montazeri A, Madah D, Shormasti NK. The comparison of cure behaviour of epoxy and multi-wall carbon nanotube/epoxy composites. J Therm Anal Calorim 2016;124:1441–8.

[21] Vijayan P P, Puglia D, Rastin H, Reza Saeb M, Shojaei B, Formela K. Cure kinetics of epoxy/MWCNTs nanocomposites: isothermal calorimetric and rheological analyses. Prog Org Coating 2017;108:75–83.

[22] Cividanes LS, Simonetti EAN, Moraes MB, Fernandes FW, Thim GP. Influence of carbon nanotubes on epoxy resin cure reaction using different techniques: a comprehensive review. Polym Eng Sci 2013;54:11.

[23] Qiu SL, Wang CS, Wang YT, Liu CG, Chen HF, Xie XY, et al. Effects of graphene oxides on the cure behaviors of a tetrafunctional epoxy resin. Express Polym Lett 2011;5:809–18.

[24] Zhou T, Wang X, Liu X, Xiong D. Influence of multi-walled carbon nanotubes on the cure behaviour of epoxy-imidazole system. Carbon 2009;47:1112–8.

[25] Reza Saeb M, Bakhshandeh E, Ali Khonakdar H, Mäder E, Scheffler C, Heinrich G. Cure kinetics of epoxy nanocomposites affected by MWCNTs functionalization: a review. Sci World J 2013:703708. https://doi.org/10.1155/2013/703708.

[26] Zhou T, Gu M, Jin Y, Wang J. Studying on the curing kinetics of a DGEBA/EMI-2,4/nano-sizedcarborundum system with two curing kinetic methods. Polymer 2005;46:6174–81.

[27] Chen W, Auad ML, Williams RJJ, Nutt SR. Improving the dispersion and flexural strength of multiwalled carbon nanotubes–stiff epoxy composites through b-hydroxyester surface functionalization coupled with the anionic homopolymerization of the epoxy matrix. Eur Polym J 2006;42:2765–72.

[28] Ma L, Zhao D, Zheng J. Construction of electrostatic and π–π interaction to enhance interfacial adhesion between carbon nanoparticles and polymer matrix. J Appl Polym Sci 2020;137(18):48633.

[29] Perumal S, Lee HM, Cheong IW. A study of adhesion forces between vinyl monomers and graphene surfaces for non-covalent functionalization of graphene. Carbon 2016;107:74–6.

[30] Zhao D, Zhu G, Ding Y, Zheng J. Construction of a different polymer chain structure to study π-π interaction between polymer and reduced graphene oxide. Polymers 2018;10(7):716.